東北大学機関リポジトリ

TOUR

Tohoku University Repository

東北大学

Estimation of the degree of hydrogen bonding between quinoline and water by ultraviolet-visible absorbance spectroscopy in sub- and supercritical water

Estimation of the degree of hydrogen bonding between quinoline and water by ultraviolet–visible absorbance spectroscopy in sub- and supercritical water

Mitsumasa Osada, Katsunori Toyoshima, Takakazu Mizutani, Kimitaka Minami, Masaru Watanabe, Tadafumi Adschiri, and Kunio Arai[a]
Department of Chemical Engineering, Tohoku University, 07 Aza-Aoba, Aramaki, Aoba-ku, Sendai, 980-8579, Japan

UV–visible spectra of quinoline was measured in sub- and supercritical water ($25\,°C < T < 430\,°C$ and $0.1\,MPa < P < 40\,MPa$), and the degree of hydrogen bonding between quinoline and water was estimated from solvatochromic shifts in the $\pi-\pi^*$ absorbance band. Hydrogen bonding decreased with increasing temperature from 25 to 360 °C. At supercritical conditions ($380\,°C < T < 400\,°C$), hydrogen bonding abruptly decreased where the isothermal compressibility of water was large ($0.5 < \rho_r < 1.5$). In this condition, local density around quinoline was lower than bulk density, namely negative solvation, and it led to the cleavage of hydrogen bonding between quinoline and water. © 2003 American Institute of Physics. [DOI: 10.1063/1.1545099]

I. INTRODUCTION

The local solvation structure around solutes in supercritical fluids can be attributed to the balance between kinetic energy of molecules and solute–solvent interactions (dispersion, induction, and dipole–dipole).[1,2] For the case of supercritical water, hydrogen bonding adds to the above-described solute–solvent interactions and is an important factor to control the solvation structure. Further, the solvent properties of water such as dielectric constant change greatly with temperature and density, which probably leads to the great change of hydrogen bonding between solute and water. Hence, the estimation of the dependence of solute–solvent hydrogen bonding and other interactions (dispersion, induction, and dipole–dipole) on temperature and water density is essential for evaluating the solvation structure in supercritical water.

UV–visible spectroscopy has been employed for the estimation of solute–solvent interactions with their solvatochromic shifts and the shifts can be represented by the physical properties of the solvent. In general, the frequency of maximum absorbance, $\nu(\max)$, can be expressed by the McRae–Bayliss expression[3] as follows:

$$\nu(\max) = A + B\frac{n^2-1}{2n^2+1} + C\left(\frac{\epsilon-1}{\epsilon+2} - \frac{n^2-1}{n^2+2}\right), \quad (1)$$

where n is the refractive index and ϵ is the dielectric constant of the solvent. The first term (A term) is $\nu(\max)$ in the condition where no solute–solvent interaction exists, such as in a vacuum. The second term (B term) is for the interaction between the solute dipole and induced dipole of the solvent, and the third term (C term) expresses the dipole–dipole interactions. These constants (A, B, and C) are correlated from spectral shift data in ordinary liquids that do not form hydro-

gen bonding to the probe. For the case where solvent forms hydrogen bonding, $\nu(\max)$ can be expressed by the Kamlet–Taft π^*, α, β scale[4] as follows:

$$\nu(\max) = A + S\pi^* + D\alpha + E\beta, \quad (2)$$

where the second term (π^* scale) is for the interactions that combine the solvent dipolarity and polarizability. The α and β scale describes the solvent hydrogen bond donor acidities, and the solvent hydrogen bond acceptor basicities, respectively. There are dual contributions of hydrogen bonding to solvatochromic shifts. The first contribution comes via the macroscopic n and ϵ, and the second contribution originates from the specific interactions between the solute and water. Because of hydrogen bonding, the dielectric constant of water is quite large as compared with other molecules with same size of dipole moment. However, this contribution works as a whole on solvatochromic shift and is therefore included in Eq. (1). On the other hand, specific hydrogen bonding interactions between the solute and water should be extracted as the difference between the experimentally obtained shifts and that can be estimated by Eq. (1). In this work, we attempted to extract the latter contribution, namely hydrogen bonding between solute and water.

In supercritical fluids, the difference between the estimated $\nu(\max)$ from Eq. (1) and the experimental $\nu(\max)$ is often observed even for solvents that do not form hydrogen bonding. Some researchers attribute this difference to the specific solvation around the solute and estimated local density around the solute.[1,2,5–35] Kajimoto[1] studied the charge transfer state formation for (N,N-dimethylamino)-benzonitrile in CF_3H and attributed the larger spectral shift to the occurrence of aggregation of solvent molecules around the solute. As the bulk density increased, the bathochromic shift asymptotically converged to that observed in the liquid phase. Kim and Johnston[5] also found local density enhancement, namely positive solvation, through UV–visible spectra of phenol blue in supercritical ethylene, chlorotrifluo-

[a]Electronic mail: karai@arai.che.tohoku.ac.jp

4573

romethane, and fluoroform. They reported that the local density to the bulk density is related linearly to the isothermal compressibility. In supercritical water, the difference probably includes the effect of hydrogen bonding between solute and solvent as well as solvation. Bennett and Johnston[6] observed UV–visible spectra of acetone in supercritical water and reported the importance of estimating the dependence of solute–solvent hydrogen bonding on temperature and water density. Lu *et al.* determined the Kamlet–Taft π^*, α, β scale of near critical water based on solvatochromic measurements and reported that the polarity and hydrogen bonding of water are highly tunable properties with temperature.[7,8] To evaluate the solvation around the solute in supercritical water, a separation of the contributions of solute–solvent hydrogen bonding and solvation is required.

The first objective of this work is to estimate the solvatochromic shifts over a wide range of temperatures (25 °C $< T < 430$ °C) and pressures (0.1 MPa $< P < 40$ MPa). The second objective is to evaluate the difference of the spectrum for the estimation and discuss the effect of hydrogen bonding between quinoline and water and the solvation structure around the quinoline. In this work, quinoline was chosen as a probe to quantify these interactions. Quinoline is the spectral probe that is stable in supercritical water (460 °C) for about 1 h,[36] and the $\pi-\pi^*$ absorbance bands are known to be sensitive to hydrogen bond interactions.[37–39]

II. EXPERIMENT

A. Materials

Distilled and de-ionized water was used with resistivity of 18.2 MΩ cm. Deoxygenation was conducted with LABOC GASTORR GT-102. Quinoline used was of 95.0% of purity from Wako Pure Chemical Industries, Ltd. Solvents used were with the highest purity available (hexane: 99.0%, heptane: 99.0%, cyclohexane: 99.5%, diethyl ether: 99.5%, isobutyl nitrile: 97.0%, DMF: 99.5%, acetonitrile: 99.0%, DMSO: 99.0%, methanol: 99.8%, and ethanol: 99.5 mol %). Carbon dioxide of 99.99 mol % was purchased from Nihon Sanso.

B. Apparatus

A flow-type apparatus was used to allow *in situ* UV–visible absorbance spectroscopic measurement in supercritical water as shown in Fig. 1. UV–visible spectra were obtained with a polychromator/spectrograph (JASCO, CT-25TP) with a 0.12 nm resolution. The spectroscopic cell was fabricated from hastelloy C-276 and contained two 8-mm diam, 5.0-mm-thick sapphire windows sealed with gold foil. The path length of the cell was 7.6 mm. The temperature of the cell was maintained at measurement temperature to an accuracy of ± 1.0 °C by a temperature controller (RKC, REX-F900) and K-type thermocouples (Sukegawa Denki, 1.6 mm o.d.) inserted directly into the cell body. The cell was heated with a thermostatic unit (JASCO, 6762-1001-KIYO). The pressure was controlled electronically with a HPLC pump (JASCO, PU-987) combined with a backpressure regulator (TESCOM, model 26) and was measured by an
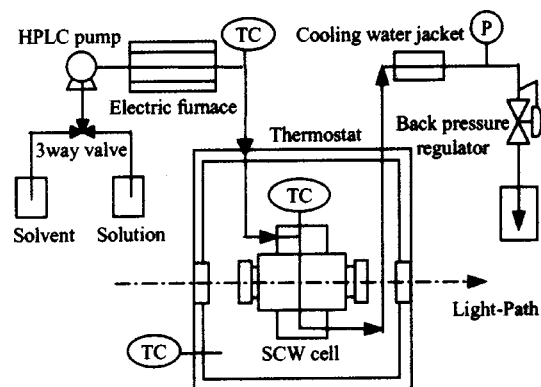

FIG. 1. Flow apparatus for transmission spectroscopy.

analog pressure gauge (NAGANO KEIKI Co.) with an accuracy of $\pm 0.15\%$ F.S.

III. METHOD FOR UV–VISIBLE MEASUREMENTS

Measurements were performed according to the following procedure. The solvent without solute was fed at 5 mL/min into the system. After the temperature and pressure fluctuations became smaller than 1 °C and 0.1 MPa, respectively, a reference spectrum of solvent was measured. Next, the quinoline solution was fed at 5 mL/min into the system, and a sample spectrum of solution was measured. An absorbance spectrum was obtained by subtracting the reference spectrum from the sample spectrum at the same temperature and pressure. The reference and sample spectrum were recorded only when baseline fluctuations were less than 0.1% in the wave number range from 30 000 to 40 000 cm^{-1}, since quantitative discussion required high reproducibility in the absorbance spectra. The concentrations (2.63, 4.18, 7.59×10^{-4} or 1.93×10^{-3} mol/L) used were well below the saturated solubility limits of quinoline in each solvent. The spectral shift also occurs by the solute–solute interaction (multimerization). It is reported that the quinoline follows Beer's law without the spectral shift in the cyclohexane solvent at the concentration from 1.00×10^{-4} to 4.32×10^{-2} mol/L at 25 °C and 0.1 MPa.[40] We observed $\nu(\mathrm{max})$ in aqueous solution at different concentrations (2.63 and 7.59×10^{-4} mol/L) from 25 to 400 °C and obtained the same $\nu(\mathrm{max})$ which absorbance could be expressed by Beer's law. Spectroscopic research in the past using quinoline was carried out at the equivalent concentration to our experiment.[37–39] In this work, we assumed that the solute–solute interactions could be neglected at our experimental concentrations.

IV. RESULTS

Figure 2 shows the $\pi-\pi^*$ absorption spectra of quinoline in water at various temperatures and 25 MPa. The signal/noise ratios of the spectrum were from 150 (360 °C) to 350 (25 °C). With an increase in temperature, the $\pi-\pi^*$ absorption band shifted to higher energies (blueshift). Figure 3 shows experimentally obtained $\nu(\mathrm{max})$ in water over a wide range of temperature versus pressure. In the liquid phase (25 °C $< T < 360$ °C), the variation of $\nu(\mathrm{max})$ with pressure was negligible, while at supercritical conditions
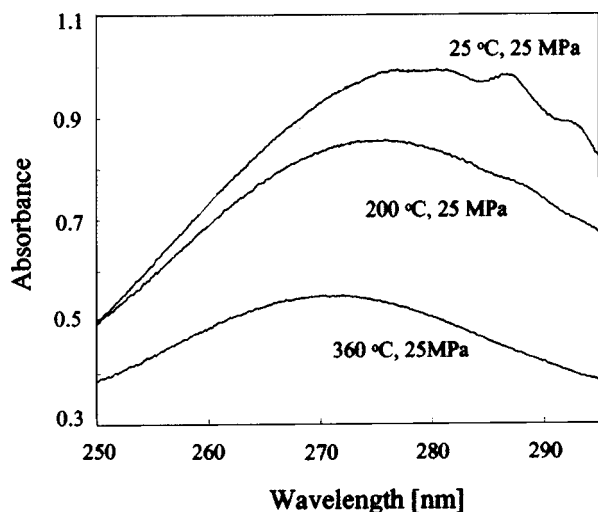
FIG. 2. The $\pi-\pi^*$ absorption spectra of quinoline in water (solute concentration 4.18×10^{-4} mol/L).

FIG. 4. Experimentally obtained values vs estimated values by A, B, C terms at 25 °C. (1) Argon, (2) CO_2 (63 °C, 8–30 MPa), (3) CO_2 (25 °C, 6–30 MPa), (4) hexane, (5) heptane, (6) cyclohexane, (7) diethyl ether, (8) isobutyl nitrile, (9) acetonitrile, (10) DMF, (11) DMSO, (12) ethanol, (13) methanol, (14) water.

(380 °C$<T<$400 °C) a significant decrease of ν(max) with increasing pressure was observed. In particular, near the critical point (380 °C$<T<$400 °C, 20 MPa$<P<$30 MPa), the decrease of ν(max) with pressure was drastic, but at high pressures, namely in the high density region, the pressure dependence became smaller. At 430 °C, namely in the low density region, the change of ν(max) with increasing pressure was smaller.

First, solute–solvent interactions (dispersion, induction, and dipole–dipole) except hydrogen bonding between quinoline and water were estimated from the spectrum shift in nonhydrogen bonding solvents or in gaseous phase (Ar, CO_2) from Eq. (1). The value of ν(max) in argon was employed as the constant A (38.0×10^3 cm^{-1}), although the accuracy of ν(max) might not be so high due to the weak spectrum in the dilute gas phase measurement. The constant B (-3.85×10^3 cm^{-1}) of the equation was correlated with the experimentally obtained ν(max) in nonpolar solvents (hexane, heptane, cyclohexane) by using refractive index (n) and dielectric constant (ϵ) of the solvent and the value of A
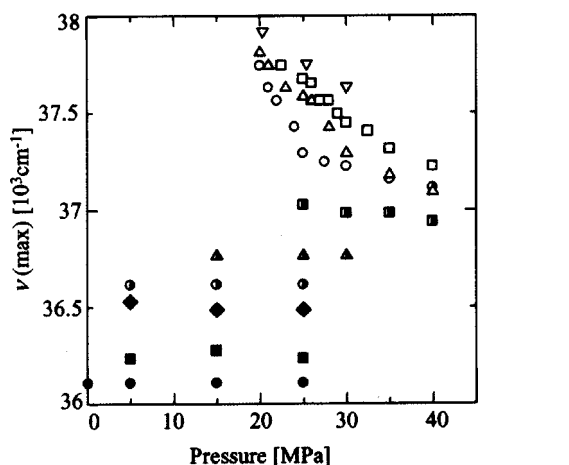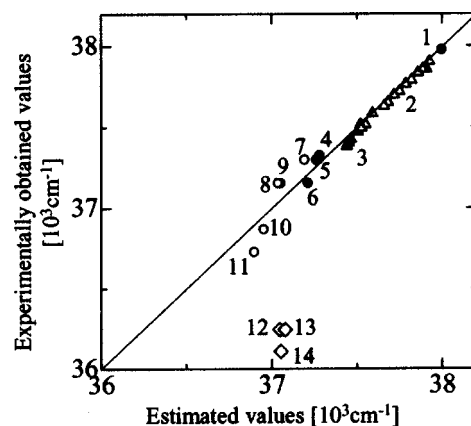
evaluated earlier. The constant C (-0.383×10^3 cm^{-1}) was correlated with experimentally obtained ν(max) in polar solvents that do not form hydrogen bonds (diethyl ether, isobutyl nitrile, acetonitrile, DMF, DMSO). In Fig. 4, the experimentally obtained values of nonhydrogen bonding solvents and argon gas were fitted to Eq. (1), with a root-mean-square deviation of about 100 cm^{-1}, which was the same order of magnitude as the experimental error in the determination of band frequencies of the solution spectra ($\sim$50 cm^{-1}).

The temperature and pressure dependence of solute–solvent interactions, except hydrogen bonding between quinoline and water, were evaluated. We measured ν(max) in gaseous argon at temperatures ranging from 25 to 300 °C at 0.1 MPa, where no change of ν(max) was observed over this temperature range. The pressure dependence was evaluated by employing CO_2 ($n^2=\epsilon$) as a solvent in a range of pressure from 8 to 30 MPa at constant temperatures of 25 and 63 °C and the correlation of Moriyoshi et al.[41] (Fig. 4). Good correlation ($R^2=0.99$) of the experimental results with the estimated values by Eq. (1) with the parameters A, B, and C evaluated earlier could be obtained. These results indicated that the effect of pressure on the A and B values was negligible at pressures up to 30 MPa. Thus, in this analysis we assumed that A, B, and C were constants irrespective of temperature and pressure.

Next, ν(max) values in hydrogen bonding solvents (methanol, ethanol, and water) were compared with the estimated values from Eq. (1) (Fig. 4). The experimental ν(max) had smaller wave numbers than the estimated ν(max). These differences, $\Delta\nu_{\text{difference}}$, for the hydrogen bonding solvents are probably due to hydrogen bonding between quinoline and solvent and may be attributed to the Kamlet–Taft α, β scale.[4]

Figure 5 shows the relation between $\Delta\nu_{\text{difference}}$ and the reduced density, ρ/ρ_c, in water over a wide range of temperatures. The bulk refractive index (n) and the bulk dielectric constant (ϵ) from the literature[42,43] were used for the estimation of ν(max) with Eq. (1). The error bars were obtained from the recalculated ν(max) values by Eq. (1) using ϵ

FIG. 3. The ν (max) of quinoline in water vs pressure. ($\bullet$) 25 °C, ($\blacksquare$) 100 °C, ($\blacklozenge$) 200 °C, ($\circledcirc$) 250 °C, ($\blacktriangle$) 300 °C, ($\boxminus$) 360 °C, ($\circ$) 380 °C, ($\triangle$) 390 °C, ($\square$) 400 °C, ($\triangledown$) 430 °C.
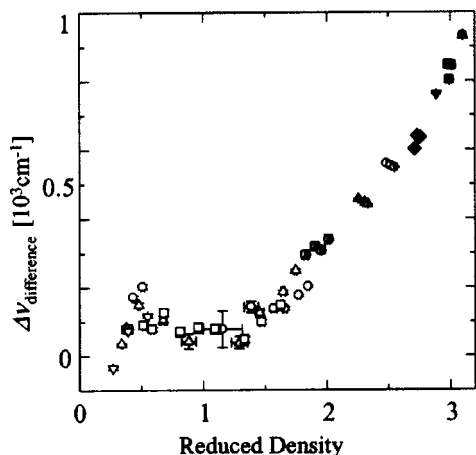
FIG. 5. The $\Delta \nu_{\text{difference}}$ in water vs reduced density. (●) 25 °C, (▲) 50 °C, (■) 100 °C, (▼) 150 °C, (◆) 200 °C, (◗) 250 °C, (△) 300 °C, (▣) 360 °C, (○) 380 °C, (△) 390 °C, (□) 400 °C, (▽) 430 °C.

and n considering both ± 1 °C temperature errors and ± 0.1 MPa pressure errors. There was a general trend of decreasing $\Delta \nu_{\text{difference}}$ with decreasing water densities.

V. DISCUSSION

Figure 6 shows $\Delta \nu_{\text{difference}}$ in supercritical CO_2 ($T_c = 31.1$ °C) in a range of pressure from 8 to 30 MPa at constant temperature of 38 °C. Error bars were given to all experimental results at ± 1 °C temperature errors and ± 0.1 MPa pressure errors. The $\Delta \nu_{\text{difference}}$ observed in supercritical CO_2 was smaller than that for supercritical water. Supercritical CO_2 is a nonhydrogen bonding solvent and thus the difference between the estimated $\nu(\text{max})$ by Eq. (1) and experimentally obtained $\nu(\text{max})$ can probably be attributed to the difference of the local ϵ and n from the bulk ϵ and n.[1,2,5–35] In supercritical CO_2, the $\Delta \nu_{\text{difference}}$ exhibited a peak in a range of $0.5 < \rho_r < 1.5$.

There are some reports that solvation occurs around the solute which has high local densities.[1,2,5–35] In this paper we refer to this solvation as "positive solvation." The estimated $\nu(\text{max})$ by Eq. (1) around the critical density is calculated to
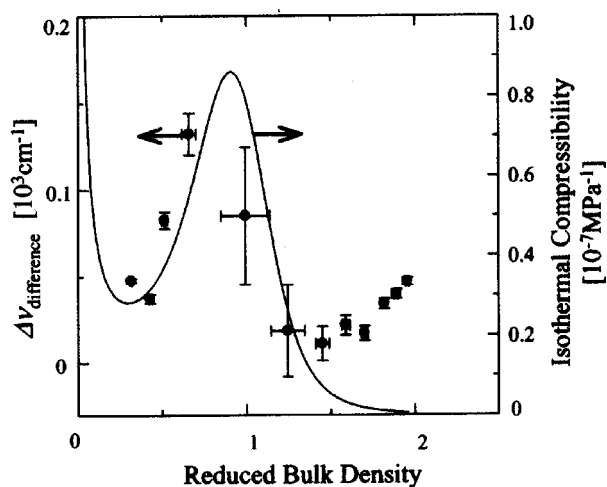

FIG. 6. The $\Delta \nu_{\text{difference}}$ in CO_2 and the isothermal compressibility vs reduced density at 38 °C.
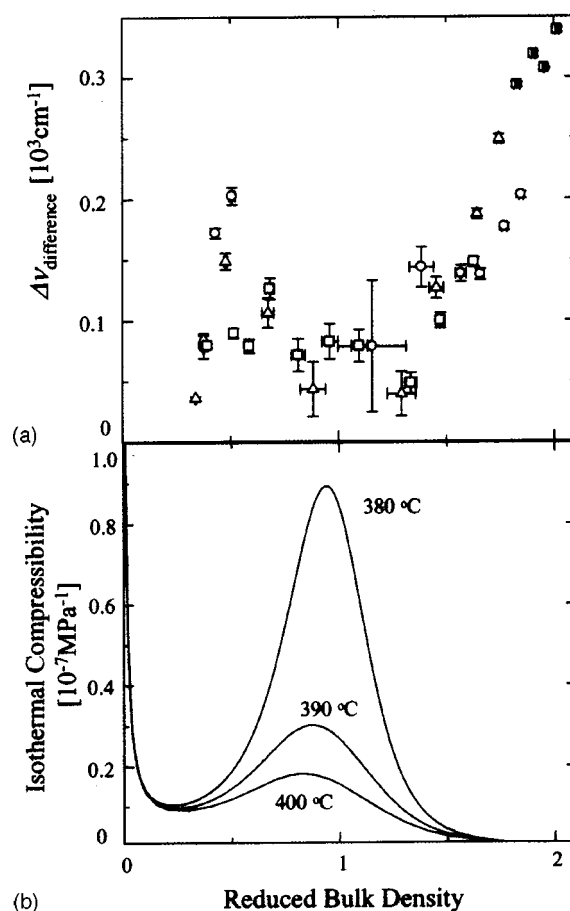

FIG. 7. (a) The $\Delta \nu_{\text{difference}}$ in water vs reduced density. (b) Isothermal compressibility. (▣) 360 °C, (○) 380 °C, (△) 390 °C, (□) 400 °C.

be smaller as compared with the correct $\nu(\text{max})$, since positive solvation gives an increase in both local n and ϵ. In the present analyses, $\Delta \nu_{\text{difference}}$ was evaluated from the bulk n and ϵ, which might underestimate the true n and ϵ, and thus lead to an overestimation in $\Delta \nu_{\text{difference}}$. Kim and Johnston[5] claimed that the effect of solvation increased with the isothermal compressibility of fluids. Figure 6 shows a comparison of $\Delta \nu_{\text{difference}}$ and the isothermal compressibility of the fluid. In supercritical CO_2, the $\Delta \nu_{\text{difference}}$ became significant where the isothermal compressibility of the fluid was large as reported by Kim and Johnston.[5] This result suggests higher local density around quinoline than the bulk. Figure 7 is a magnification of Fig. 5 with the isothermal compressibility of water. The data shown in Fig. 7 exhibited a sigmoidal shape. In a range of $1 < \rho_r < 2$, the $\Delta \nu_{\text{difference}}$ decreased as the ρ_r decreased. Just below the critical density ($0 < \rho_r < 1.0$), $\Delta \nu_{\text{difference}}$ became larger with decreasing density, but then became smaller again at low densities. The peak appearing in the range of density for $0 < \rho_r < 1.0$ was largest at 380 °C and decreased with increasing temperature. Although there is experimental error in the data, in supercritical water the maximum peak of $\Delta \nu_{\text{difference}}$ ($0 < \rho_r < 1.0$) was observed at lower density region than the maximum of isothermal compressibility ($0.5 < \rho_r < 1.5$). This trend is different from that observed in supercritical CO_2 in Fig. 6.

The solvation structure around the solute is attributed to the competition between the solvent–solvent interaction and

the solute–solvent interaction. There are three types of solvation in supercritical conditions according to molecular dynamics studies.[44] The first is positive solvation, which is defined as the case where local density is higher than the bulk. The second is weak positive solvation, which is defined as the case where local density is slightly higher than the bulk density. The third is negative solvation, which is defined as the case where local density is lower than the bulk. For the case of nonpolar supercritical CO_2 solvent, quinoline–CO_2 forces are probably higher than that for CO_2–CO_2 forces. However, the affinity of quinoline with water is lower than the water–water interactions. This leads to the probable negative solvation around a quinoline in water.

Although the mechanism of this result has not yet been elucidated, the following hypothesis of negative solvation may be one of the probable explanations. Since quinoline molecule is hydrophobic, water molecules do not preferentially allocate themselves or solvate around quinoline molecules, although solvation may occur in the vicinity of the nitrogen atom. Thus, at a lower density region ($0 < \rho_r < 0.5$), a kind of positive solvation occurs around the nitrogen atom of quinoline molecules. However, hydrogen bonding between nitrogen atom of quinoline and hydrogen atom of water is weaker than that between water molecules. Thus, at the near critical density region where isothermal compressibility is high, water molecules gathered each other rather than solvated around the nitrogen atom of quinoline. The assembly of water molecules formed especially in the near critical regions ($0.5 < \rho_r < 1.5$). This assembly of water molecules attracted solvated water molecules around the nitrogen atom of quinoline. Thus, the cleavage of hydrogen bonding between quinoline and water occurred. At high density region ($1.5 < \rho_r$) hydrogen bonding formed between the nitrogen atom of quinoline and the hydrogen atom of water, because the bulk density of water molecules was as high as that of local solvation shell.

VI. CONCLUSION

Solvatochromic shifts in the $\pi - \pi^*$ absorption band of quinoline show a strong relationship between hydrogen bonding and other solute–solvent interactions (dispersion, induction, and dipole–dipole) in supercritical water. The degree of hydrogen bonding between quinoline and water decreased with increasing temperature from 25 to 360 °C. In supercritical water, the degree of hydrogen bonding between quinoline and water decreased in water density especially around the critical point. In the critical region, lower local density around quinoline than bulk density, namely negative solvation, was observed.

ACKNOWLEDGMENT

[1] O. Kajimoto, Chem. Rev. **99**, 355 (1999).
[2] S. C. Tucker, Chem. Rev. **99**, 391 (1999).
[3] E. G. McRae, J. Phys. Chem. **61**, 562 (1957).
[4] M. J. Kamlet, J. L. M. Abboud, and R. W. Taft, *Progress in Physical Organic Chemistry* (Wiley, New York, 1981), Vol. 13; C. Reichardt, *Solvent Effects in Organic Chemistry* (Chemie, Weinheim, 1988).
[5] S. Kim and K. P. Johnston, Ind. Eng. Chem. Res. **26**, 1206 (1987).
[6] G. E. Bennett and K. P. Johnston, J. Phys. Chem. **98**, 441 (1994).
[7] J. Lu, J. S. Brown, E. C. Boughner, C. L. Liotta, and C. A. Eckert, Ind. Eng. Chem. Res. **41**, 2835 (2002).
[8] J. Lu, J. S. Brown, C. L. Liotta, and C. A. Eckert, Chem. Commun. (Cambridge) **7**, 665 (2001).
[9] J. Lu, B. Han, and H. Yan, Ber. Bunsenges. Phys. Chem. **102**, 695 (1998).
[10] K. Takahashi, K. Abe, S. Sawamura, and C. D. Jonah, Chem. Phys. Lett. **282**, 361 (1998).
[11] B. L. Knutson, S. R. Sherman, K. L. Bennett, C. L. Liotta, and C. A. Eckert, Ind. Eng. Chem. Res. **36**, 854 (1997).
[12] D. Schwarzer, J. Troe, and M. Zerezke, J. Chem. Phys. **107**, 8380 (1997).
[13] K. P. Hafner, F. L. L. Pouillot, C. L. Liotta, and C. A. Eckert, AIChE J. **43**, 847 (1997).
[14] C. R. Yonker and R. D. Smith, J. Phys. Chem. **92**, 235 (1988).
[15] J. F. Kauffman, J. Phys. Chem. A **105**, 3433 (2001).
[16] J. E. Lewis, R. Biswas, A. G. Robinson, and M. Maroncelli, J. Phys. Chem. B **105**, 3306 (2001).
[17] R. Biswas, J. E. Lewis, and M. Maroncelli, Chem. Phys. Lett. **310**, 485 (1999).
[18] E. D. Niemeyer and F. V. Bright, Energy Fuels **12**, 823 (1998).
[19] E. D. Niemeyer, R. A. Dunbar, and F. V. Bright, Appl. Spectrosc. **51**, 1547 (1997).
[20] J. K. Rice, E. D. Niemeyer, R. A. Dunber, and F. V. Bright, J. Am. Chem. Soc. **117**, 5832 (1995).
[21] Y. Sun, J. Am. Chem. Soc. **115**, 3340 (1993).
[22] Y. Sun, G. Bennett, K. P. Johnston, and M. A. Fox, J. Phys. Chem. **96**, 10001 (1992).
[23] J. F. Brennecke, D. L. Tomasko, J. Peshkin, and C. A. Eckert, Ind. Eng. Chem. Res. **29**, 1682 (1990).
[24] A. Morita and O. Kajimoto, J. Phys. Chem. **94**, 6420 (1990).
[25] P. Lalanne, S. Rey, F. Cansell, T. Tassaing, and M. Besnard, J. Supercrit. Fluids **19**, 199 (2001).
[26] N. Wada, M. Saito, D. Kitada, R. L. Smith, Jr., H. Inomata, K. Arai, and S. Saito, J. Phys. Chem. B **101**, 10918 (1997).
[27] M. Kanakubo, T. Umecky, H. Kawanami, T. Aizawa, Y. Ikushima, and Y. Masuda, Chem. Phys. Lett. **338**, 95 (2001).
[28] M. Kanakubo, T. Aizawa, T. Kawakami, O. Sato, Y. Ikushima, K. Hatakeda, and N. Saito, J. Phys. Chem. B **104**, 2749 (2000).
[29] S. Bai, C. M. V. Taylor, F. Liu, C. L. Mayne, R. J. Pugmire, and D. M. Grant, J. Phys. Chem. B **101**, 2923 (1997).
[30] F. G. Baglin, S. K. Murray, J. E. Daugherty, T. E. Palmer, and W. Stanbery, Mol. Phys. **98**, 409 (2000).
[31] S. A. Egorov, J. Chem. Phys. **113**, 7502 (2000).
[32] J. L. deGrazia, T. W. Randolph, and J. A. O'Brien, J. Phys. Chem. A **102**, 1674 (1998).
[33] F. J. P. Schuurmans, D. T. N. de Lang, G. H. Wegdam, R. Sprik, and A. Langedijk, Phys. Rev. Lett. **80**, 5077 (1998).
[34] J. E. Lewis, R. Biswas, A. G. Robinson, and M. Maroncelli, J. Phys. Chem. B **105**, 3306 (2001).
[35] T. Aizawa, Y. Ikushima, N. Saitoh, K. Arai, and R. L. Smith, Jr., Chem. Phys. Lett. **357**, 168 (2002).
[36] A. R. Katritzky, R. A. Barcock, M. Siskin, and W. N. Olmstead, Energy Fuels **8**, 990 (1994).
[37] M. F. Anton and W. R. Moomaw, J. Chem. Phys. **66**, 1808 (1977).
[38] N. Mataga and S. Tsuno, Bull. Chem. Soc. Jpn. **30**, 368 (1957).
[39] N. Mataga, Y. Kaifu, and M. Koizumi, Bull. Chem. Soc. Jpn. **29**, 373 (1956).
[40] K. R. Hall, R. C. Wilhoit, K. N. Marsh, A. M. Ferguson, and B. Boyed, *Selected Ultraviolet Spectral Data/Thermodynamics Research Center Hydrocarbon Project*, Vol. 3, Serial No. 958 (Thermodynamics Research Center, Texas Engineering Experimental Station, Texas A & M University, College Station, 1945–1977).
[41] T. Moriyoshi, T. Kita, and Y. Uosaki, Ber. Bunsenges. Phys. Chem. **97**, 589 (1993).
[42] P. Schiebener, J. Straub, J. M. H. Levelt Sengers, and J. S. Gallagher, J. Phys. Chem. Ref. Data **19**, 677 (1990).
[43] M. Uematsu and E. U. Franck, J. Phys. Chem. Ref. Data **9**, 1291 (1980).
[44] I. B. Petsche and P. G. Debenedetti, J. Chem. Phys. **91**, 7075 (1989).